# Repair of Pier Bridge Model Post-Earthquake

## Innino Justitiannisa[1], Riawan Gunadi[1]

[1]Faculty of Civil Engineering,
 Politeknik Negeri Bandung, Bandung, 40599, INDONESIA

*Corresponding Author

**Abstract:** This study concentrates on the bridge pier model which was damaged by the earthquake and repaired using grouting and carbon wrapping materials. This research consists of a one pier bridge model with two steps of testing, namely step 1 in the form of a cyclic test of the pier bridge model which will be followed by step 2 in the form of structural repairs with grouting and carbon wrapping materials and retesting to evaluate the performance of the structural repair technology used. This research will show the cyclic test results using the repair material applied to the same sbr latex concrete material test object. The test object used is a pier bridge model with dimensions of 0.25×0.25×1.68 meters. The material specifications used are concrete f'c 30, fy 400 MPa deformed longitudinal reinforcement and stirrups fy 240 MPa. The test was carried out with a constant axial load of 0.2.f'c.Ag and a cyclic lateral load. Structural performance analysis was carried out according to ACI 374.1-05. Step 1 cyclic test was carried out until the drift ratio was 3.5%. The lateral peak strength achieved was 8.606 tonf with indications of shear damage indicated by the number of cracks in the web area. The second step of the cyclic test was carried out to a drift ratio of 6.25% with a lateral peak strength of 8.640 tonf with indications of flexural damage. Cyclic test results show that repair with a grouting material and carbon wrap can restore peak strength, deformation capacity, and stiffness degradation.

**Keywords:** Pier, cyclic lateral load, repair, grouting materials, carbon wrapping

## 1.  Introduction

Indonesia has a high potential for earthquakes. In 2017, Indonesia experienced twenty-three destructive earthquakes, and in 2018 twenty-three times [1]. The bending properties of bridge pier/column elements when subjected to lateral compressive forces are influenced by the axial compressive forces acting on them so that they make up most of the pier strengths in carrying axial compressive forces, thereby decreasing the bending response and affecting the low ductility and dissipation energy. Bridge piers can experience progressive collapse during a large earthquake due to low ductility when the displacement is inelastic [2].

When an earthquake occurs at the end of the pier, the bridge suffers damage in the form of cracks or breaks in the concrete [3]. One of the damages to the bridge piers is caused by shear failure. The presence of diagonal cracks in the pier area indicates the shear failure that occurs. Diagonal cracks on the pier, if left unrepaired (not repaired), can continue until the structure collapses [4]. The use of concrete materials in the implementation of construction often experiences damage such as cracks (cracks), cavities (cavities or holes), and corrosion that occurs in the reinforcement [5]. The damage causes the structure to experience a decrease in performance, so an improvement that can restore the structure is needed. Many alternatives can be used to repair damaged structures, including steel jackets, RC jackets, fibre-reinforced polymer (FRP) jackets, grouting, wrapping, patching, and so on [3]. The repairs carried out help restore the strong performance of the pier structure due to cyclic loads to prevent more fatal damage to the bridge pier structure when it experiences an earthquake.

## 2.1 Repair

Repair or retrofit of a structure is carried out when there is a decrease in performance, which causes the technical requirements to be no longer met, namely strength, stiffness, stability, and resistance to environmental conditions (durability). The term repairing is applied to damaged buildings that have experienced a loss of strength, so they need to be returned to their original state [6].

The repair can be interpreted as restoring or increasing the strength and stiffness of damaged structural elements so that they can withstand the load again as planned. Structures that have changed the function of buildings are designed according to old regulations with the use of low nominal earthquake loads, and even the previous structure was only designed for gravity loads without considering the possibility of seismic loads that might cause damage or even structural failure so that repairs are needed [5].

## 2.2 Grouting

Grouting is a process of inserting cement paste into the cracks in cracked concrete [7]. Estogrout MP 70 is a grouting material with several advantages, including being unable to shrink, providing high flexural and compressive strength performance, and being able to bind very strongly to steel and concrete. Estogrout MP 70 contains microsilica, which can increase the strength and durability of concrete [8]. This grouting material comes from PT. Hissan Indonesia with specifications that can be seen in Table 1.

**Table 1 - Estogrout MP 70 specifications**

| Property | 1 day (N/mm$^2$) | 7 day (N/mm$^2$) | 28 day (N/mm$^2$) |
|---|---|---|---|
| Compressive Strength | > 30 | > 55 | > 70 |
| Flexural Strength | > 5 | > 9 | > 11 |
| Time for Expansion | 15 mins to 2 hours | | |
| Fresh Weight Density | 2179 kg/m$^3$ | | |
| Young's Modulus | 28 kN/mm$^2$ | | |
| Expansion Characteristics | 0.5-2.0% | | |

## 2.3 Wrapping

Carbon wrapping is a repairing material used in reinforced concrete by applying non-metallic composite materials in cloth-like sheets. Carbon fibre is a fibre that contains at least 90% carbon by weight. Carbon fibre shows no corrosion or cracking at room temperature. The function of repair with the CFRP system is to increase strength or provide increased flexural, shear, axial, and ductility capacities. The way to install CFRP is to wrap it around the surface of the reinforced structural element using an epoxy resin adhesive. The working system is the same as conventional transverse reinforcement [6]. Carbon wrapping has several advantages, including being more accessible to install, having high tensile strength, and can be installed on concrete, steel, or wood surfaces. Carbon wrap is usually applied as shear reinforcement in columns and beams. Estowrap 300 is a packing material in carbon fibre sheets with high tensile strength and modulus of elasticity. EstoWrap 300 was specially developed by PT. Hissan Indonesia. EstoWrap 300 can improve the structure's performance by strengthening and increasing the shear strength [8]. Estowrap 300 specifications can be seen in Table 2 and Fig. 1.

**Table 2 - EstoWrap 300 specifications**

| EstoWrap 300 | |
|---|---|
| Tensile Strength | 4900 N/mm$^2$ |
| Ultimate Strength | 4.900 MPa |
| Fiber Stiffness | 230 GPa |
| Density | 1.8 - 2.0 g/cm$^3$ |
| Elongation | 2.10% |
| Elasticity Modulus | 230 GPa |
| Rapture Strength | 2.5 % |

**Fig. 1 - Carbon wrapping [12]**

## 2.4 Cyclic Test

Cyclic loads are repeated loads received by a structure [9]. Based on SNI 7834-2012, the cyclic test is a process in which the test object is loaded with a cyclic load and uses a displacement control method representing the expected floor deviation at the joint during an earthquake. The cyclic test is carried out with three complete cycles with increasing deviation. The initial deviation ratio should be within the specimen's linear elastic behaviour range. Drift ratios are intended to ensure that the displacement increases gradually in steps that are neither too large nor too small [10].

## 2.5 Stiffness

According to ACI 374.1-05, To provide adequate initial stiffness, the test model must achieve a lateral load equal to or greater than the nominal lateral load (En) before the drift ratio exceeds the initial drift ratio consistent with the permissible drift limits of IBC 2000. The initial stiffness is calculated as a drift ratio equal to $\Delta a / \phi.C.dh$ where $\phi$ is the strength reduction factor according to the conditions, bending or shear, which controls the design of the test module by 0.9. For $\Delta a/h$ equal to 0.015, a Cd deflection amplification factor of 5.5 is required [11]. The initial stiffness is calculated based on the hysteretic curve at the last drift ratio after the load is stopped in the third cycle, as shown in Fig. 2.
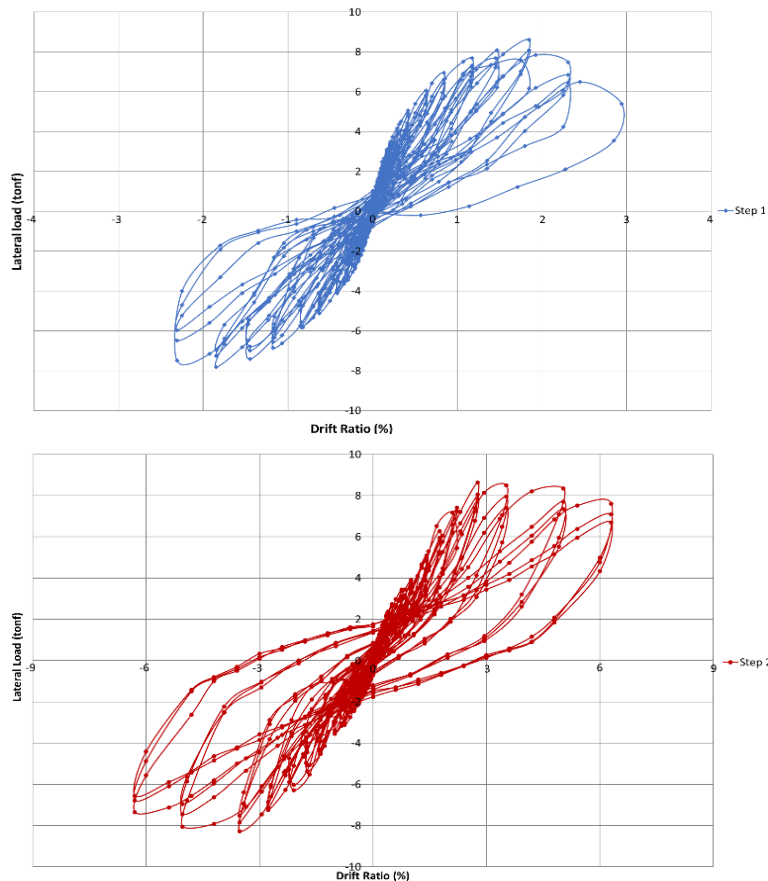


**Fig. 2 - Hysteretic curve**

## 2.6 Peak Strength

Peak strength (Emax) is the maximum lateral load of the model specimen determined from the test results. Peak strength can be obtained from the maximum lateral load before softening conditions on the load-displacement graph presented in the backbone curve. Peak strength can be seen in Fig. 3.
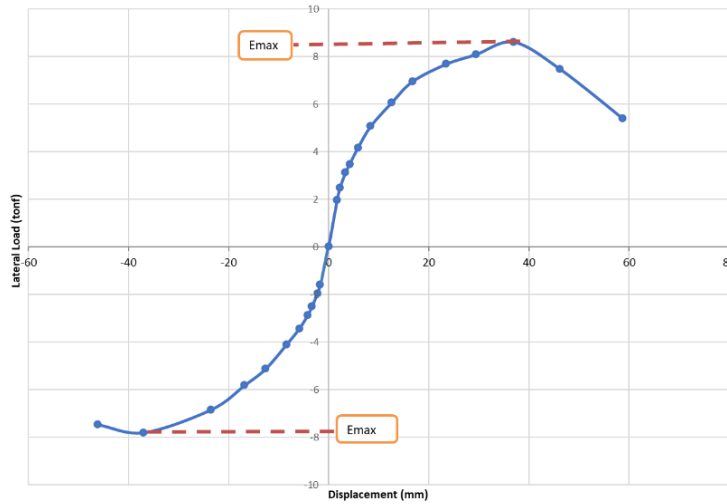


**Fig. 3 - Peak strength**

## 2.7 Deformation Capacity

The deformation capacity is calculated when the lateral load is terminated in softening condition or not less than 75%Emax. The deformation capacity can be seen in Fig. 4.
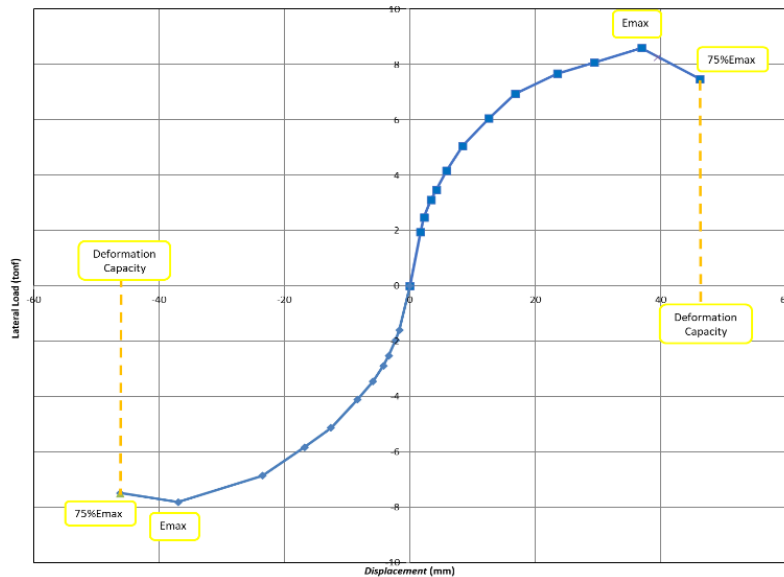


**Fig. 4 - Deformation capacity**

## 2.8 Energy Dissipation

Energy dissipation is the ability of a structure to absorb energy in the plastic area. When a cyclic load is applied to a structure, the energy absorbed in one cyclic load is the amount of energy absorbed when receiving a tensile load and a compressive load. The total energy dissipated during loading is the area (hysteresis loop) of the third cycle for each drift ratio value [12]. This study's energy dissipation calculation uses the ACI 374.1-05 concept, as shown in Fig. 5, expressed by the following equation.

$$\beta = \frac{\Delta_h}{\left(E_1 + E_2\right)\left(\theta'_1 + \theta'_2\right)}$$

(1)

203
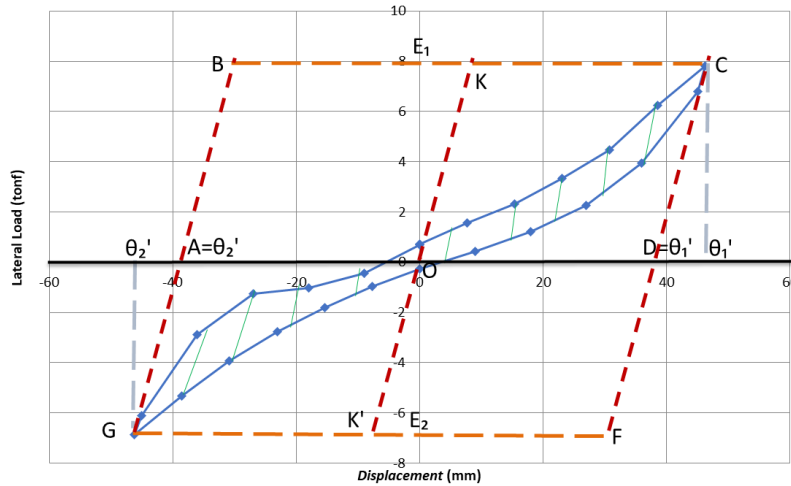
**Fig. 5 - Energy dissipation**

## 3. Methodology

This research was conducted on one test object, a bridge pier model consisting of two testing steps. Step 1 is in the form of a cyclic test of the bridge pier model, and step 2 is in the form of structural repairs and re-testing to evaluate the performance of the structural repair technology used. The cyclic test was carried out according to ACI-374-1-05. The specimen will be loaded with static axial force and lateral force. The cyclic loading given to the test object is carried out constantly until the test object collapses. The results of this study in the form of initial stiffness, peak strength, deformation capacity, energy dissipation, and stiffness degradation are used as parameters to evaluate the effectiveness of repair technology. The research flowchart can be seen in Fig. 6.
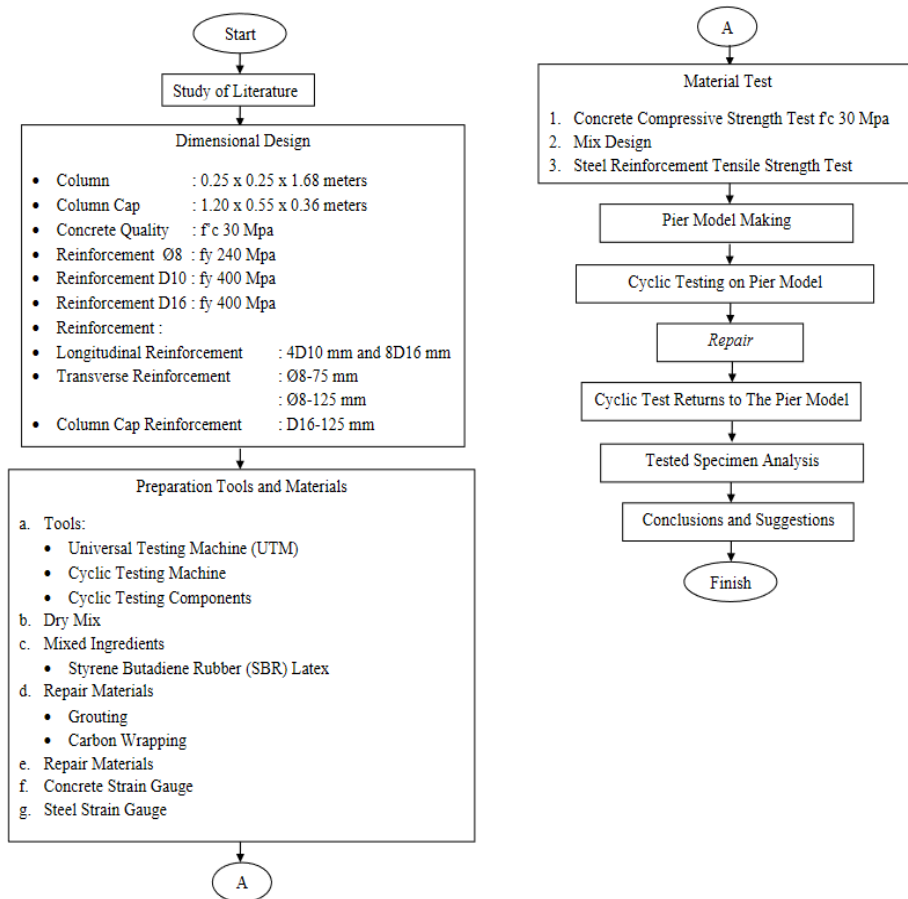


**Fig. 6 - Flowchart**

## 3.1 Pier Model Design

In this study, the property and geometry data for the pier model were determined based on previous experiments conducted by Puji et al. [10]. The bridge pier model was made in one piece with a column cap size of 1200 mm long, 550 mm wide, 360 mm high, and 250 mm × 250 mm pier cross-sectional dimension with a height of 1860 mm. In this study, the designed concrete was f'c = 30 MPa. The quality of the reinforcing steel was fy = 400 MPa with the number of longitudinal bars 4D10 and 8D16, and the grade of steel for the transverse reinforcement was 240 MPa with a diameter of reinforcement Ø8mm with a distance between bars of 75 and 125 mm. Fig.7 is a complete specification of the test object as follows.
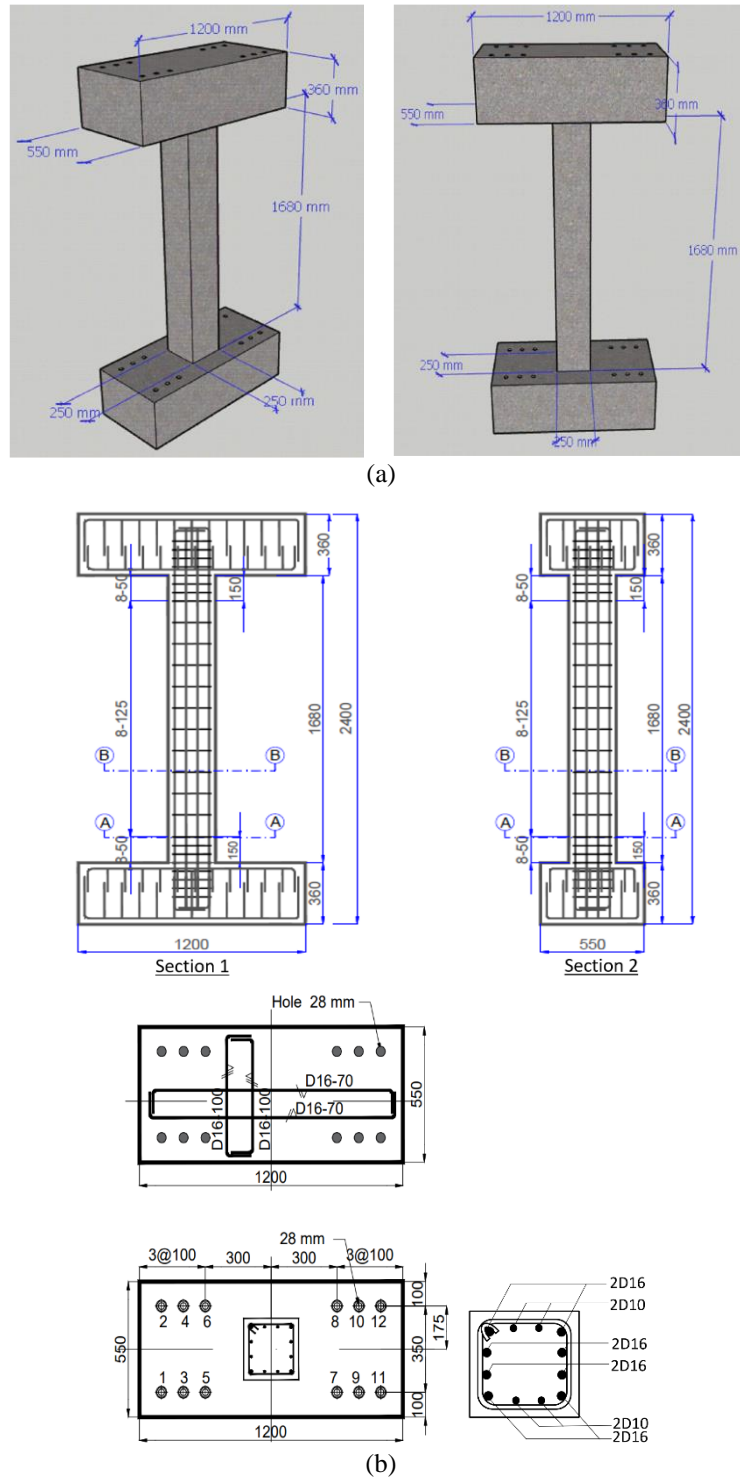


**Fig. 7 - Pier models (a) illustration of pier model, and; (b) details of cross-sectional reinforcement of the model**

## 3.2 Instrumental Testing

Cyclic testing follows ACI-374-1-05. The pier model specimen is mounted on the loading frame. Furthermore, the pier model specimen is installed with Linear Variable Displacement to identify the displacement at several pier points when the lateral load is applied. The load used is a static axial load of 30 tonf, and a lateral load is a cyclic displacement. The load is given in the form of displacement in an alternating direction. In the early step, the load is set so the structure behaves linearly elastic. For each deviation value given in three cycles, the deviation increase is given by 0.25 - 0.5 times compared to the previous deviation. The cyclic test is stopped at a load level of about 80% of the peak load so that the specimen is in a softening condition. Fig. 8 below shows the loading pattern. Tool settings, test illustrations, and locations of cyclic testing LVDTs can be seen in Fig. 9.
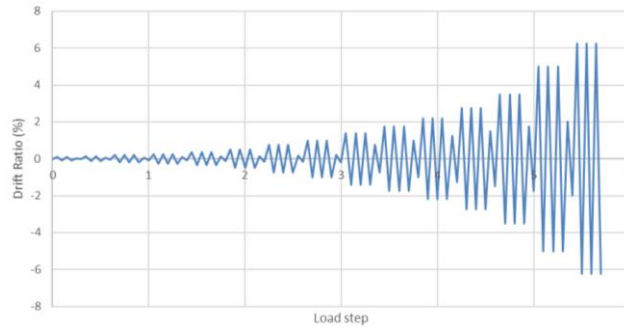


**Fig. 8 - Cyclic lateral loading pattern**



(a)
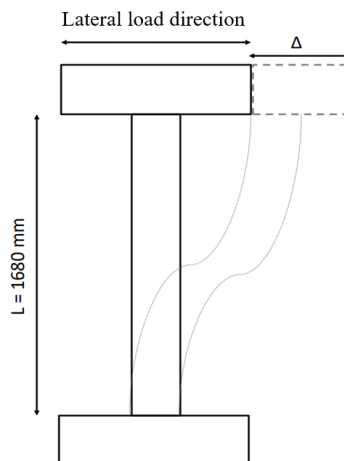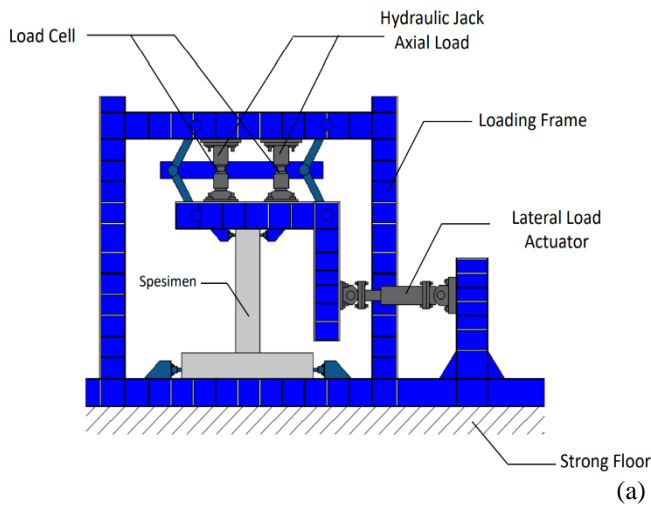


**Fig. 9 - Set-up of pier model (a) schematic of test setup, and; (b) ilustration of cyclic testing**

## 4. Results and Discussion

This test was carried out experimentally on a pier model with two steps of testing, including the first step of the cyclic test and the second step, namely the repair of damaged specimens due to the first step of the cyclic test and another cyclic test. Cyclic test results will be analyzed based on ACI 374.1-05. The use of ACI 374.1-05 in this test as a comparison is taken by the parameters in it to analyze the cyclic test results on the pier model in the first and second steps of testing. This is because ACI 374.1-05 should be applied to buildings, but in this test, ACI 374.1-05 is used for bridges. The following is an analysis of the results of the first and second steps of testing.

### 4.1 Stiffness

The initial stiffness ($K_o$) is the ratio between the force and the displacement at the initial lateral load with the hysterical slope of the curve at the displacement interval +0.35% to -0.35% drift ratio. In contrast, the stiffness degradation is determined from the stiffness secant in the third cycle when the last drift ratio is tested. Stiffness reduction is taken into account where the stiffness of the secant connecting the point is a drift ratio of -0.0035 to a drift ratio of +0.0035. The initial stiffness results are represented in Table 3 and Fig. 10. The results of the Stiffness calculations for the two test phases are shown in Table 4 and Fig. 11.

Test results on the second step of the pier model have a lower initial stiffness than the first step test, namely 94.92% of the push direction and 71.98% of the pull direction. The test results show that the second step of stiffness degradation has a higher rate of 111.16% in the push direction and 26.73% in the pull direction compared to the first step testing the pier model.

**Table 3 - Initial stiffness in the pier model**

| Step | Loading Condition | Drift Ratio (%) | $\Delta_a$ (mm) | $E_a$ (tonf) | $K_o$ (tonf/mm) |
|---|---|---|---|---|---|
| (1) | (2) | (4) | (5) | (6) | (7) = (6)/(5) |
| I | Push (+) | 0.303% | 5.50 | 3.958 | 0.7196 |
| | Pull (-) | 0.303% | 5.50 | 3.224 | 0.5862 |
| II | Push (+) | 0.303% | 5.50 | 2.030 | 0.3692 |
| | Pull (-) | 0.303% | 5.50 | 1.875 | 0.3401 |
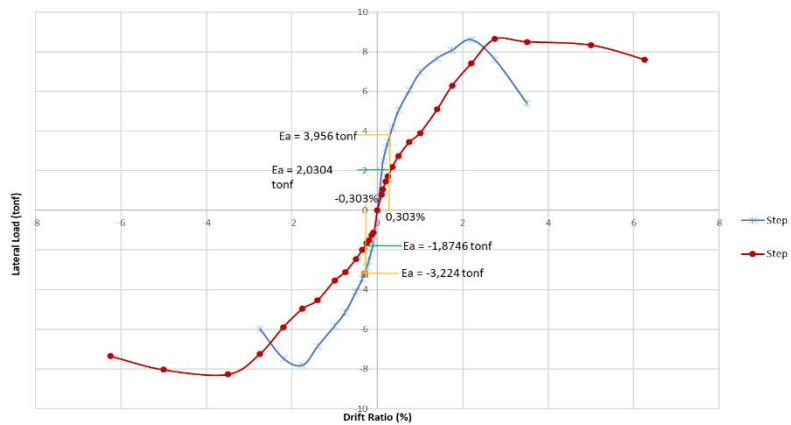


**Fig. 10 - Initial stiffness**

**Table 4 - Stiffness degradation in the pier model**

| Step | Loading Condition | Initial Stiffness $K_o$ (tonf/mm) | Displacement difference at 0.35% (mm) | Load difference at 0.35% (tonf) | Stiffness at drift ratio0.35%, K' (tonf/mm) | Ratio K'/ $K_o$ (tonf/mm) |
|---|---|---|---|---|---|---|
| (1) | (2) | (3) | (4) | (5) | (6) | (7) = (6)/(3) |
| I | Push (+) | 0.72 | 11.76 | 1.20 | 0.1020 | 14.17 |
| | Pull (-) | 0.59 | 11.76 | 0.95 | 0.0808 | 13.69 |
| II | Push (+) | 0.37 | 11.76 | 1.30 | 0.1105 | 29.86 |
| | Pull (-) | 0.34 | 11.76 | 0.70 | 0.0595 | 17.50 |

(a)



(b)
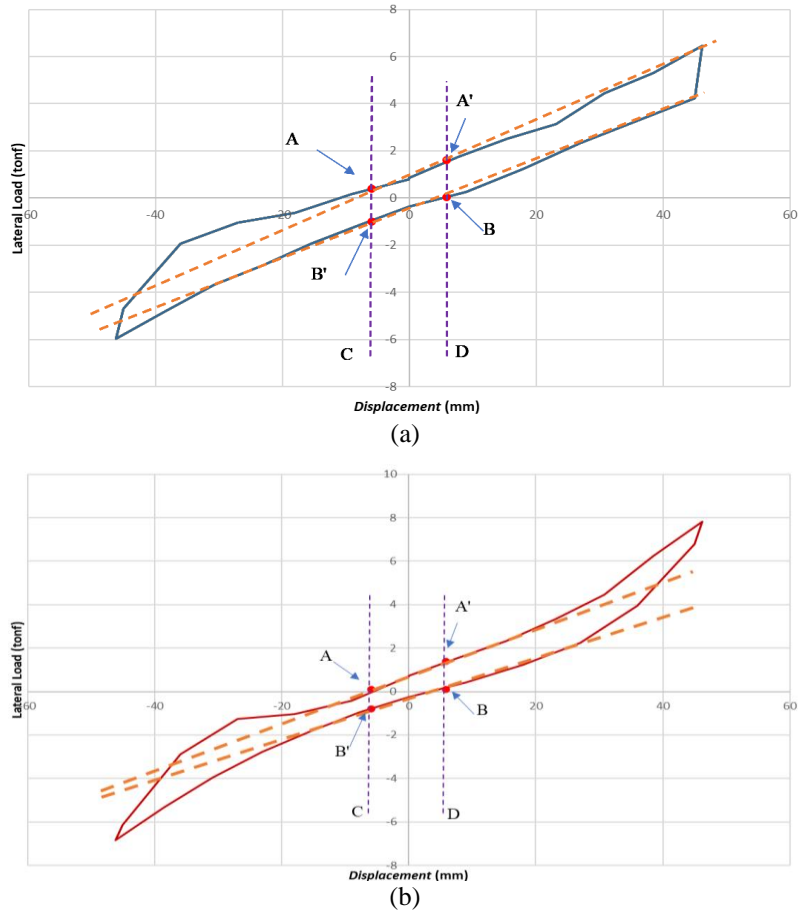
**Fig. 11 - Stiffness degradation (a) hysteresis curve for stiffness degradation of first step pier model (A = 0,4 tonf; A' = 1,6 tonf; B = 0,05 tonf; B' = -1 tonf; C = -5,88 mm; D = 5,88 mm), and; (b) hysteresis curve for stiffness degradation of second step pier model (A = 0,1 tonf; A' = 1,4 tonf; B = 0,1 tonf; B' = -0.8 tonf; C = -5,88 mm; D = 5,88 mm)**

## 4.2 Peak Strength

The magnitude of the peak strength is obtained from the peak lateral load (Emax) on the load-displacement graph presented in the backbone curve. The peak strength is observed when the maximum load has been reached before experiencing strength degradation (softening condition). The peak load in this test can be seen in Fig.12. Fig. 12 shows that the pier model in the second step has a higher peak strength than the first step of testing, which is 0.39% in the push direction and 5.93% in the pull direction.
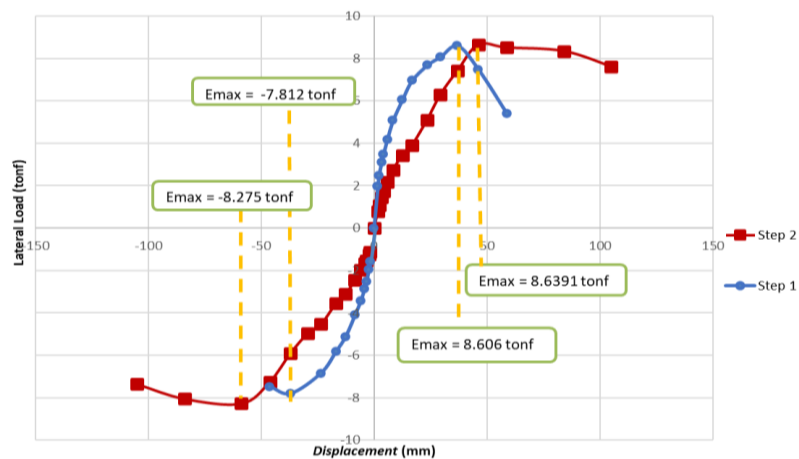


**Fig. 12 - Backbone curve for peak stiffness of the pier model in the first step and the second step**

208

## 4.3 Deformation Capacity

According to ACI 374-1-05, specimens tested with cyclic loads are required so that the deformation capacity occurs when the deformation capacity of the specimen is not less than 75% of the maximum lateral load (Emax) value in the same loading direction. The deformation capacity at both steps of this test can be seen in Table 5 and Fig.13.

**Table 5 - Deformation capacity in the pier model**

| Step | Maximum Push (+) | | Maximum Pull (-) | | Maximum Load | Eu/ Emax ≥ 0.75Emaks |
|------|------------------|--|------------------|--|--------------|----------------------|
| | $E_u$ (tonf) | $\Delta u$ (mm) | $E_u$ (tonf) | $\Delta u$ (mm) | Emaks (tonf) | (%) |
| I | 8,626 | 39,5 | | | 8,606 | 96 |
| | | | 7,481 | 39,5 | 7,812 | 96 |
| II | 8,294 | 87,1 | | | 8,640 | 96 |
| | | | 7,944 | 88 | 8,275 | 96 |



**Fig. 13 - Backbone curve for deformation capacity of the pier model the first step and the second step**

Tests at the two steps that have been carried out show that the results of the deformation capacity on the pier model are not less than 0.75Emax in the push and pull directions, as seen in Fig. 13. The second step of testing shows a higher deformation capacity than the first step of testing, namely 120, 51% in the pushing direction and 90.476% in the pulling direction.

## 4.4 Energy Dissipation

The energy dissipation of the pier model at each drift ratio level is calculated as the area of the loop cycle (shaded area). The area of the loop in each loading cycle can be calculated based on the difference in the displacement values that occur multiplied by the average load value. Energy dissipation is defined as the area of the ABCD parallelogram, where the results of calculating the loop area for both test steps are presented in Table 6 and Fig. 14. Based on Table 6, it can be seen that the cumulative dissipation energy in the second step is smaller than in the first step which is equal to 18.66%.

**Table 6 - Relative energy dissipation ratio in the pier model**

| Step | The area of the shaded region (tonf.mm) | The area is limited by ABCD and DFGA (tonf.mm) | Relative energy dissipation ratio, β |
|------|------------------------------------------|------------------------------------------------|--------------------------------------|
| (1) | (2) | (3) | (4) = (2)/(3) |
| I | 205.0015 | 1146.9150 | 17.87 |
| II | 204.0915 | 1354.8890 | 15.06 |

(a)



(b)
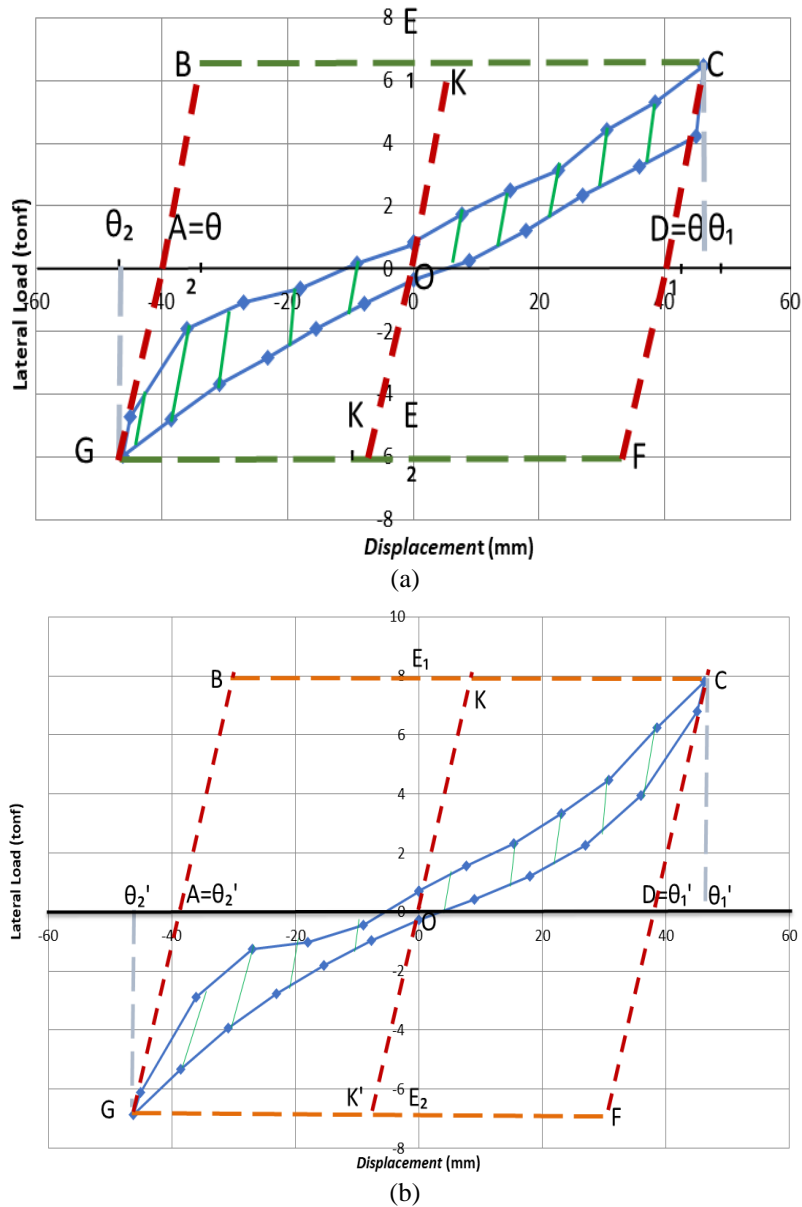
**Fig. 14 - Stiffness degradation (a) hysteresis curve at drift ratio 2.75% cycle to 3 for energy dissipation first step pier model, and; (b) hysteresis curve at drift ratio 2.75% cycle to 3 for energy dissipation second step pier model**

## 4.5 Damage Pattern

At the initial loading of the cyclic test in the first step, a relatively small lateral load is given so that the first crack has not formed. Then, the lateral load was increased so that the pier specimen experienced the first crack in the form of a micro crack at the base of the pier when the drift ratio was 0.20%. It starts with a shear crack on the right side of the pier surface and develops on each side of the pier. Shear cracks dominate the crack pattern that occurs in the pier. The cracks that occur continue to increase along with the increase in the load given to the pier test object. Extension or widening of the crack appears in the test object's pier in the first step of the test when the load increases to approach the maximum load. The crack width was still very small before the drift ratio was 3.5%. When the drift ratio was increased to 3.5%, the strength of the pier continued to grow until the pier dropped and the concrete cover began to peel off (cover spalling). The pier model first experienced cracks at the column's bottom with a shear crack pattern, followed by a flexural crack. These shear cracks occur primarily in the column base area to a height of about 50 cm - 100 cm from the column base. Testing of the pier model reached the limit at a load of 8.606 tonf with a displacement of 36.96 mm (drift ratio 2.20%). When the test object was almost destroyed, the cracks got longer and broader, appearing in new places on the sides of the pier. When the load reaches the maximum pier, it collapses suddenly. The damage in the first step resulted in a decrease in the structural performance of the pier model. The damage to the pier model in the first step of testing can be seen in Fig. 15.

In the first step, the pier model experienced a decline in structural performance, so to restore structural performance, repairs were carried out by grouting and wrapping materials to restore structural performance. In the first step, the damaged pier model, which had experienced a decline, was repaired to restore or improve performance. After the pier model has been repaired, it continues with the second stage of testing. The second stage of testing uses the same pier model as the first stage pier model, which has been repaired. The second stage of testing on the pier model, which was repaired by grouting and wrapping the cracks or cover spalling caused by the first stage of testing showed damage to the end of the pier on the front side of the pier, which was marked by fine tears in the dressing that spread to the side of the pier and cracks in the direction transverse. Flexural cracks dominate these cracks. The test object experienced the first crack, which occurred at a drift ratio of 1%. The cracks start from a drift ratio of 1% to 6.25% with marked fine tears in a transverse direction. The pier model specimen experienced the first crack at the column base with a flexural crack pattern. These flexural cracks occur mainly in the column base area to a height of about 30 cm - 50 cm from the column base. Testing the second step of the pier model resulted in an ultimate load occurring at a load of 8.640 tonf with a deflection of 46.20 mm (drift ratio 2.75%). The damage to the pier model in the second step of testing can be seen in Fig.16.
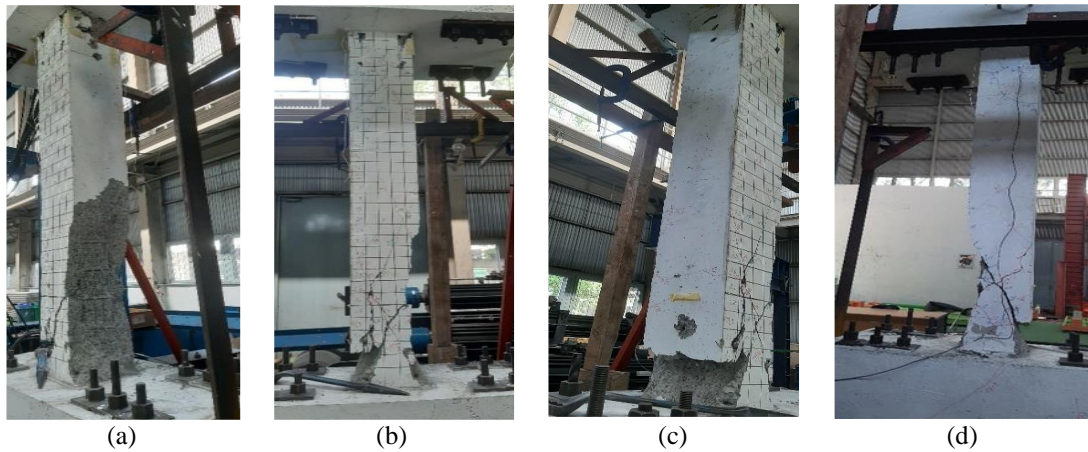


**Fig. 15 - Damage pattern in the first step of testing: (a) left side, (b) front side, (c) right side, and (d) back side**
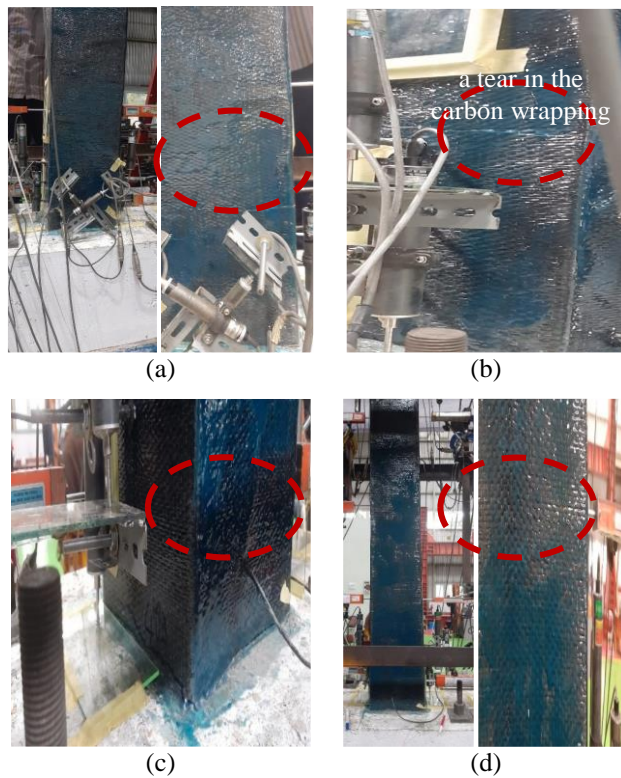


**Fig. 16 - Damage pattern in the second step of testing: (a) front side; (b) right side; (c) left side, and; (d) back side**

## 5. Conclusions

The initial stiffness in the second step of testing decreased from the initial stiffness of the first step, 94.92% in the direction of push and 71.98% in the direction of pull. From the results of the calculation analysis in the second step of testing, the pier model increased the peak strength by 0.39% in the direction of thrust and 5.93% in the direction of pull. The second step of testing experienced an increase in deformation capacity of 120.51% in the push direction and 90.476% in the pull direction compared to the first step of testing. The energy dissipation generated by the pier model in the second test was lower than in the first test by 18.66%. The pattern of damage that occurred on the pier model test object in the pier testing step was dominated by shear cracks, which were characterized by oblique/diagonal cracks from the ends of the pier that spread to all sides and along the height of the pier which caused pier cracks that exceeded the thickness of the concrete cover. Meanwhile, in the second step of testing, the pier model was dominated by flexural cracks characterized by transverse prominent cracks at the ends of the columns marked by fine tears in the wrap. The results of the second step of testing showed that improvements in grouting and wrapping could restore and even increase the peak strength and deformation capacity compared to the first step test but could not restore the initial stiffness.

## Acknowledgement

## References

[1] BMKG (2019). Katalog Gempa Bumi Signifikan dan Merusak 1821-2018. Badan Meteorologi Klimatologi dan Geofisika, pp. 13-40.

[2] Rahman M. J., Budiono B., Surono A. & Pane I. (2015). Program Eksperimental perilaku siklik pier persegi berongga jembatan dengan beton berkekuatan ultra tinggi. Jurnal Teoretis dan Terapan Bidang Rekayasa Sipil, 114, 99-113.

[3] Wu R. Y. & Pantelides C. P. (2017). Rapid seismic repair of reinforced concrete bridge columns. ACI Structural Journal, 114, 1339-1350.

[4] Kati R. R. (2016). Perilaku Lentur Balok Beton Bertulang dengan Perkuatan Geser Menggunakan Lembaran CFRP. Tugas Akhir, Universitas Hasanuddin.

[5] Afredo D., Hutomo K., Sudjarwo P. & Buntoro J. (2014). Analisa penyebab dan metode perbaikan yang tepat pada beton yang disebabkan oleh faktor non struktural. Jurnal Dimensi Pratama Teknik Sipil, 3,1-5.

[6] Mansur M. S. (2018). Perkuatan Struktur Akibat Penambahan Lantai Menggunakan Carbon Fiber Reinforced Polymer (CFRP) Dengan Studi Kasus Gedung SMP 5 Muhamadiyah Surabaya. Tugas Akhir, Institut Teknologi Sepuluh November.

[7] Udiana I. M. (2013). Desain campuran semen dan air pada pekerjaan grouting proyek bendungan/waduk nipah Madura-Jawa Timur. Jurnal Teknik Sipil, 2, 93-104.

[8] Denka Group (2017). EstoWrap. https://hissan.co.id/images/pages/products/files/estoptdsmsds/tds/Concrete Repair/ESTOP_TDS_EstoWrap_020320.

[9] Parmo (2017). Kekuatan dan daktilitas perpindahan kolom pendek beton bertulang persegi dibawah pengaruh pembebanan siklik. Jurnal Ilmu-Ilmu Teknik, 10, 42-54.

[10] SNI 7834:2012 (2012). Metode Uji Dan Kriteria Penerimaan Sistem Struktur Rangka Pemikul Momen Beton Bertulang Pracetak Untuk Bangunan Gedung. Badan Standardisasi Nasional.

[11] ACI 374.1-05. (2005). Acceptance Criteria for Moment Frames Based on Structural Testing and Commentary. American Concrete Institute.

[12] Masdiana, Parung H., Tjaronge H. M. & Djamaluddin R. (2016). Studi Eksperimental sambungan balok model takik terhadap perilaku joint interior pracetak akibat beban siklik. Prosiding Seminar Nasional Teknik Sipil, pp. 401-407.

[13] Tavio & Benny K. (2009). Desain sistem rangka pemikul momen dan dinding struktur beton bertulang tahan gempa. Media Teknik Sipil, https://onesearch.id/Record/IOS3601.slims-2129/TOC.

[14] Kurniawan P., Sumargo & Oesman M. (2021). Behavior of low-strength reinforced concrete column strengthened with carbon fiber reinforced polymer subjected to cyclic lateral load. Atlantis Press, pp. 316-323.

[15] Triwiyomo A. & Wikana I. (2000). Kuat Geser Kolom Beton Bertulang Penampang Lingkaran yang Diperbaiki dengan Metode Concrete Jacketing. Universitas Gadjah Mada.